

Response to reviewer #1

We thank the reviewer for those supportive and thoughtful comments. Our responses to the comments are provided below in blue, with the reviewers' comments in black.

General Comments:

In this study, a combined DMA-CPMA-CPC system was applied to characterize the size-resolved particle effective density in Multiphase chemistry experiment in Fogs and Aerosols in the North China Plain (McFAN) in autumn 2019. They identified a frequent bimodal distribution of particle effective density, and a unique low-density mode (named sub-density mode) accounted for ~20-30% of total observed particles. The diurnal variations of particle effective density and the influence of pollution and secondary aerosols were discussed. They concluded that the influence of BC on the effective density is even stronger than SIA.

Overall, the paper is well-written and is appropriate for ACP. The results clearly indicate the factors that govern the variations of particle effective density. The size-resolved particle effective density shown in the manuscript is interesting and would have implications for further studies. Some minor comments are still needed to be addressed before the manuscript can be published.

Response:

Thank you for the positive feedback and helpful suggestions. We have addressed the comments and implemented all suggestions in the revised manuscript as detailed below.

Specific Comments

1. The authors directly linked the sub-density mode to fresh black carbon (BC) emissions. Some organics might also have very low densities, which might lead to ambiguous conclusions. Previous measurements have also indicated that organics dominated in smaller size ranges. This is a key requirement when clarify the significance of BC in such mode.

Response:

Thanks for the comment. We agree with the reviewer that some organics might have very low densities and contribute to the sub-density mode. Therefore, we tried to assess the possible contribution of BC and organics on the sub-density mode via the correlation analysis between the number fraction of the sub-density mode (F_{sub}) and the mass fractions of BC and organics in PM_{10} . Unfortunately, there was no measurement of the chemical composition of ultrafine particles (diameter < 100 nm) during our experiment and we could not determine the actual contribution of organics in the sub-density mode at 50 and 100 nm. Accordingly, we have added this discussion in Sect. 3.1 as: *“On the other hand, a low effective density mode (density < 1.20 g cm⁻³) exists or even dominates in the measurements near emission sources, which is ascribed to freshly emitted particles and non-uniformly mixed particles (Nosko and Olofsson, 2017; Olfert and Rogak, 2019; Park et al., 2003). Numerous studies have found low effective densities of freshly emitted BC, with a minimum of 0.10 g cm⁻³ (Pagels et al., 2009). While the density of OA is usually assumed as 1.2-1.3 g cm⁻³ in most cases (Hallquist et al., 2009), some studies have found it could be as low as 0.6-1.1 g cm⁻³ (Nakao et al.,*

2011; Li et al., 2016). To elucidate the role of these two components in the sub-density mode, we further analyze the correlation between the number fraction of the sub-density mode (F_{sub}) and the mass fractions of BC and OA. As seen in Fig. S6-S7, the mass fraction of BC shows significant correlation with F_{sub} at 150, 220 and 300 nm ($R^2 = 0.46-0.57$), whereas barely no correlation is observed between OA and F_{sub} ($R^2 = 0.02-0.09$), implying that the sub-density mode at these three sizes could be mainly attributed to freshly emitted BC and the quantity of the sub-density mode is closely related to the variation of BC mass fraction. However, F_{sub} at 50-100 nm shows little correlation with either BC or OA mass fraction, which could be explained by the difference between the PM_{10} bulk chemical composition and the chemical composition of particles smaller than 100 nm.”

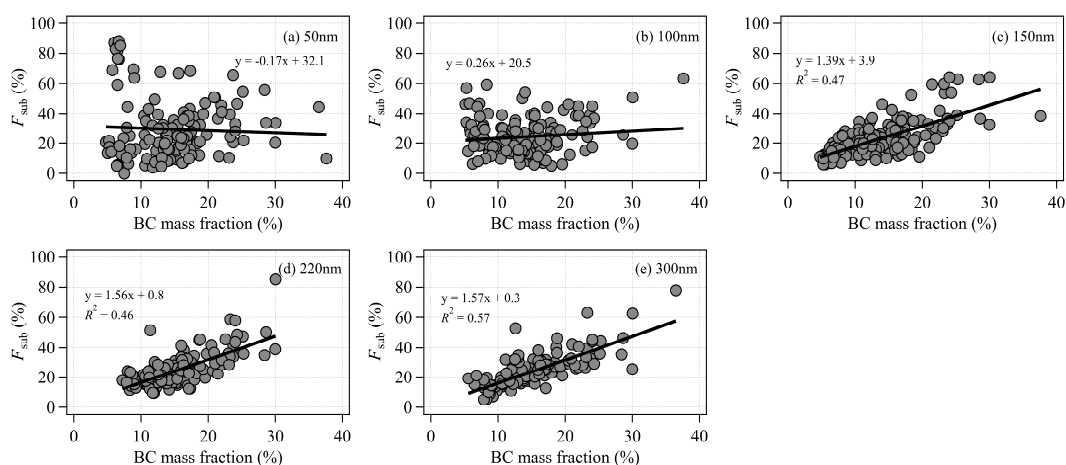


Figure R1 (S6). Correlation between BC mass fraction and the number fraction of the sub-density mode (F_{sub}) for (a) 50 nm, (b) 100 nm, (c) 150 nm, (d) 220 nm, and (e) 300 nm particles.

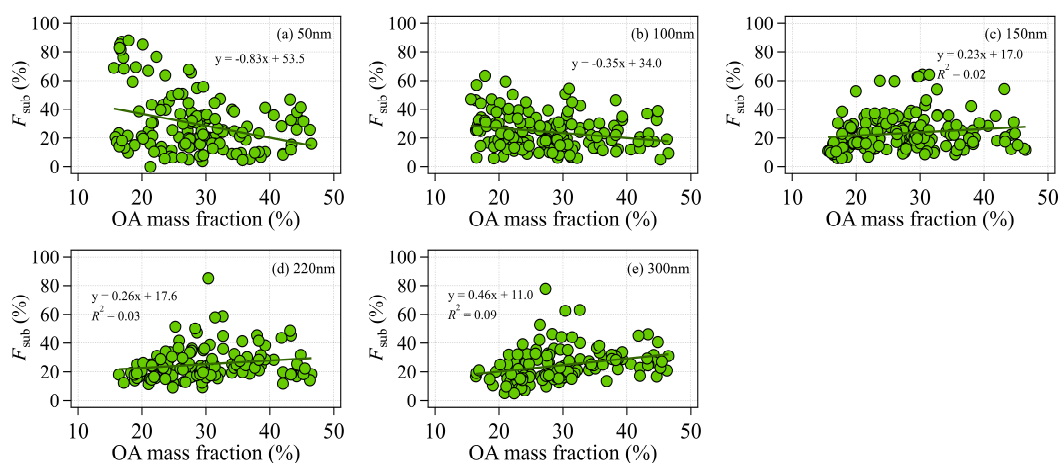


Figure R2 (S7). Correlation between OA mass fraction and the number fraction of the sub-density mode (F_{sub}) for (a) 50 nm, (b) 100 nm, (c) 150 nm, (d) 220 nm, and (e) 300 nm particles.

2. It would be better to include uncertainty data when expressing the mean density in the abstract.

Response:

Thanks for the suggestion. Following the reviewer's suggestion, we have added the standard deviation of the entire measurement when expressing the measured values in the abstract as: *"The geometric mean for the main-density mode ($\bar{\rho}_{eff,main}$) increases from $1.18\pm 0.10 \text{ g cm}^{-3}$ (50 nm) to $1.37\pm 0.12 \text{ g cm}^{-3}$ (300 nm) due to larger fraction of high-density components and more significant restructuring effect at large particle sizes, but decreases from $0.89\pm 0.08 \text{ g cm}^{-3}$ (50 nm) to $0.62\pm 0.12 \text{ g cm}^{-3}$ (300 nm) for the sub-density mode ($\bar{\rho}_{eff,sub}$) which could be mainly ascribed to the agglomerate effect of BC."*

3. abstract: "...for the sub-density mode ($\bar{\rho}_{eff,sub}$) ascribed to the agglomerate effect." Does it refer to the agglomerate effect of BC?

Response:

Yes, it refers to the agglomerate effect of BC. To make it clear, the sentence has been revised as *"...but decreases from $0.89\pm 0.08 \text{ g cm}^{-3}$ (50 nm) to $0.62\pm 0.12 \text{ g cm}^{-3}$ (300 nm) for the sub-density mode ($\bar{\rho}_{eff,sub}$) which could be mainly ascribed to the agglomerate effect of BC."*

4. Line 113: "A combined DMA-CPMA-CPC system was employed to measure the size-resolved effective density of particles with mobility diameter of 50, 100, 150, 220, and 300 nm" what is the uncertainty for the size selection?

Response:

Thanks for the comment. The sizing uncertainty of DMA and the overall measurement uncertainty of the DMA-CPMA-CPC system were evaluated using polystyrene latex (PSL) particles. A description of the uncertainties has been added in Sect. 2.1 as: *"The measurement uncertainty of the DMA-CPMA-CPC system could come from two aspects: the size classification of DMA and the mass classification of CPMA. Based on the test using polystyrene latex (PSL) particles with diameters of 150, 220, and 300 nm, an average sizing uncertainty of $\pm 2 \%$ was determined for our DMA (Fig. S4). This uncertainty is similar to the value of $\pm 1 \%$ ($\pm 1 \text{ nm}$) reported by Mulholland et al. (1999) for the size range of 100-300 nm at an aerosol-sheath flow rate ratio of 0.1. The uncertainty of the mass classification of CPMA is estimated as 1.4 % according to the results of Taylor and Kuyatt (1994) and Symonds et al. (2013). The overall measurement uncertainty of the DMA-CPMA-CPC system were also evaluated using PSL particles with diameter of 150, 220, and 300 nm before and after the field campaign. An uncertainty within $\sim 5 \%$ was found by comparing the measured effective densities with PSL material density (1.05 g cm^{-3}) (Fig. S5)."*

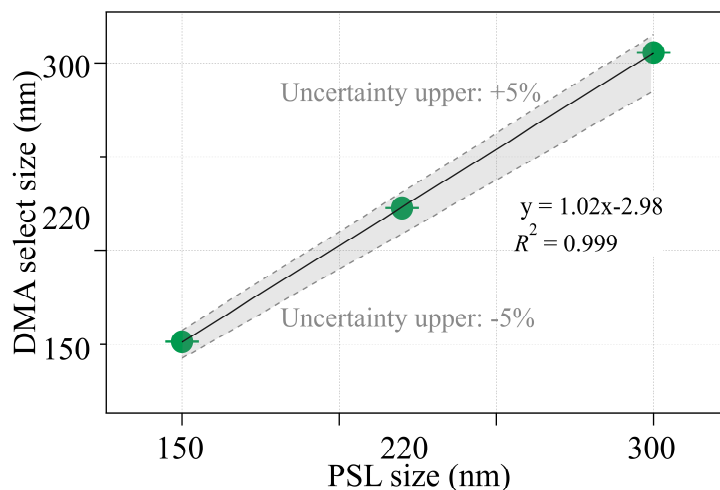


Figure R3 (S4). Uncertainty of DMA size selection.

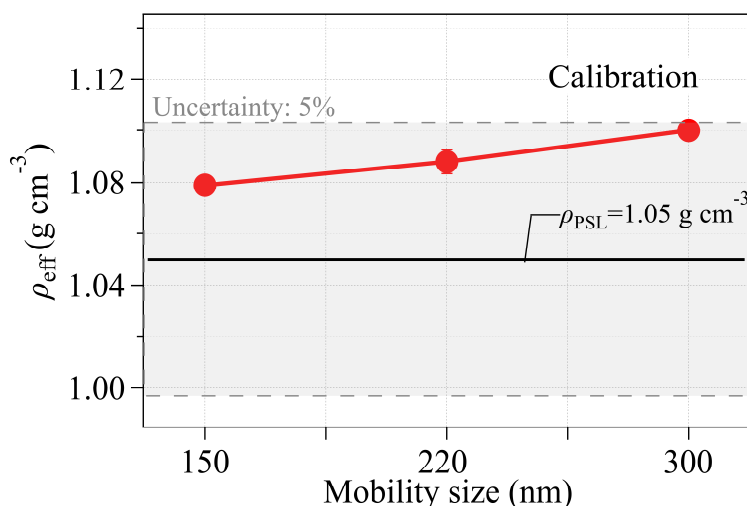


Figure R4 (S5). Calibration results for DMA-CPMA-CPC system.

5. Line 142-: It is necessary to show the uncertainty during the peak fitting with a flexible Gaussian fit algorithm, and thus potential contribution to the overall uncertainties.

Response:

Thanks for the comment. The reviewer suggested an important point for evaluating the performance of flexible Gaussian fit algorithm. We have evaluated the uncertainty of the flexible Gaussian fit algorithm and added a description in Sect. 2.2 as: “*The uncertainty of each individual Gaussian fit could be estimated based on the variation of the fitted $\bar{\rho}_{eff,i}$ in each mode at the 95 % confidence level. And the overall uncertainty is estimated by averaging the uncertainties of all the fits, which gives averages within 2.5 % and 7.0 % for $\bar{\rho}_{eff,main}$ and $\bar{\rho}_{eff,sub}$ at the five measured sizes, respectively. This uncertainty range is similar to the measurement uncertainty discussed in Sect. 2.1.*”

6. Line 205-: “The remarkably high occurrence of the sub-density mode in our study indicates a frequent influence of local BC emission.” Can these sub-density mode be matched to the variations of BC concentration?

Response:

Yes, this could be inferred by the well correlation between the area fractions of the sub-density mode (F_{sub}) with the BC mass fraction in PM_{10} (Fig. R1). As raised in Comment #1 about the possible contribution of organics to the sub-density mode, we have now revised the corresponding paragraph to include the discussion about the role of BC and organics in the sub-density mode by performing correlation analysis between F_{sub} and the mass fractions of BC and OA in PM_{10} . Please see details in the response to Comment #1.

7. Line 309: “It indicates that photochemical aging process is very efficient in transiting particles from fractal to compact morphology.” In my opinion, the conclusion can only be obtained when the pollution during daytime and nighttime is at the same level. As discussed in the previous section, the pollution level over the study is highly varied, and thus the authors should compare the increase rate of D_f under the similar conditions.

Response:

We thank the reviewer for the comment. We have now also estimated the increase rate of D_f under different pollution levels (categorized by $\text{PM}_{0.7}$ volume concentration) to minimize the influence of pollution level on the transiting particles from fractal to compact morphology. As shown in Fig. R5 (added as Fig.S16 in SI), a higher D_f increase rate at noon compared with night-time was observed at both the more polluted and the less polluted levels (Table R1, added as Table 3 in the revised manuscript), implying that photochemical aging process is very efficient in transiting particles from fractal to compact morphology.

The detailed discussion about the increase rate of D_f under different pollution levels has been added in Sect. 3.4 as: “It is worth noting that the increase rate of D_f differs between noon and night, being $\sim 0.12 \text{ h}^{-1}$ at noon which is twice of the night-time increase rate (0.06 h^{-1}). To minimize the influence of pollution level on the transiting particles from fractal to compact morphology, the variation of D_f under the more polluted and the less polluted periods was further examined separately. As shown in Fig. S16, similar diurnal variations were observed at two different pollution levels, with a higher D_f increase rate at noon than night-time (Table 3), implying that photochemical aging process at noon is very efficient in transiting particles from fractal to compact morphology. It should be pointed out that there is no D_f data during 12:00-17:00 under the more polluted condition, likely due to the transition of the sub-density mode particles to the main-density mode associated with active aging processes. Given that D_f of the more polluted period is consistently 0.20 higher than the less polluted condition (Fig. S16) and aerosol aging process at noon is very active, the D_f increase rate from 11:00 to 13:00 under the more polluted condition is calculated by assuming a D_f of 3.0 at 13:00.”

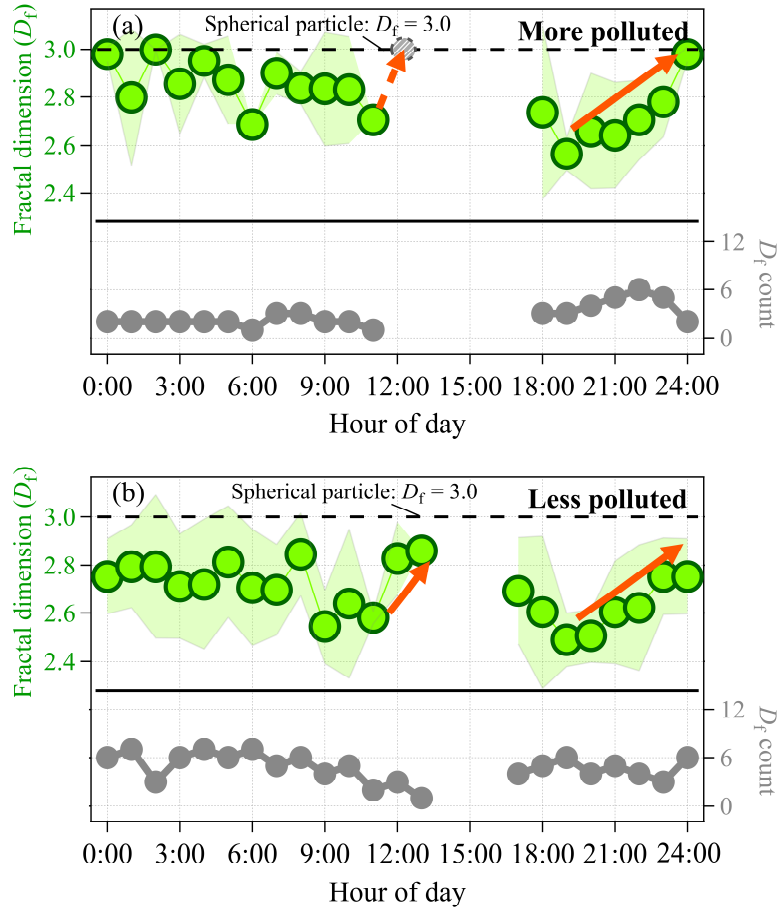


Figure R5 (S16). Diurnal cycle of fractal dimension (D_f) of the sub-density mode particles and D_f count under (a) the more and (b) the less polluted conditions. The dotted line is D_f with the value of 3.0, indicating particle with a spherical morphology. The orange arrows represent D_f with increasing trend. The grey dotted circle in the top figure represents the assumption of $D_f = 3.0$ at 13:00.

Table R1 (3). Comparison of fractal dimension (D_f) of the sub-density mode particles at noon and at night under the more and the less polluted conditions.

	D_f at 11:00	D_f at 13:00	Increase rate (h^{-1})	D_f at 19:00	D_f at 24:00	Increase rate (h^{-1})
All	2.62	2.86	0.12	2.51	2.80	0.06
More polluted	2.71	—	0.145*	2.56	2.98	0.08
Less polluted	2.58	2.86	0.14	2.49	2.75	0.05

* is calculated by assuming D_f at 13:00 is 3.0.

8. Section 4.4: Is it possible to assume a diurnal variation of BC density for the test in Figure 6, according to the source's strength of BC?

Response:

The source strength of BC exhibits not only diurnal cycle but also day-to-day variations. In the absence of detailed information on local emissions of BC and possible contribution from regional/long-range transport, it is quite difficult to directly assume a diurnal variation of BC effective density that accounts for the combination effects of different BC sources. Therefore, we tried an alternative method in which the BC effective density is retrieved for every three-hour of the day. The retrieved BC effective density does show some diurnal variation. However, due to the relatively small range of the diurnal variation as well as the marginal effect of the diurnal cycle on the correlation between $\bar{\rho}_{\text{eff,tot},300\text{nm}}$ and $\rho_{\text{eff,ACSM}}$, we still adopt a fixed BC effective density of 0.60 g cm^{-3} for the $\rho_{\text{eff,ACSM}}$ calculation in the revised manuscript.

We have thus added the corresponding discussion (also Fig. S18 and Fig. S19) about the diurnal variation of BC density in Sect. 3.5 as: “*Since strong diurnal variation was observed for BC mass fraction (Fig. S14) driven by the changes in primary source emissions, we also conduct a sensitivity analysis to retrieve BC effective density for every 3-hour of the day. The retrieved BC effective density indeed shows a diurnal pattern (Fig. S18), with high values in the afternoon and night and relatively low values during the morning and evening, which matches well with the diurnal pattern of F_{sub} (Fig. 5). However, the range of the diurnal variation ($0.52\text{-}0.64 \text{ g cm}^{-3}$) is relatively small. When applying this diurnal pattern of BC effective density in the calculation of $\rho_{\text{eff,ACSM}}$, only a marginal increase was found in the R^2 of the correlation between $\bar{\rho}_{\text{eff,tot},300\text{nm}}$ and $\rho_{\text{eff,ACSM}}$ (R^2 increased from 0.62 to 0.65, Fig. S19), probably due to the limited amount of data in each time interval and the use of bulk chemical composition in the calculation. Therefore, a fixed BC effective density of 0.60 g cm^{-3} is used for the $\rho_{\text{eff,ACSM}}$ calculation in the following analysis.*”

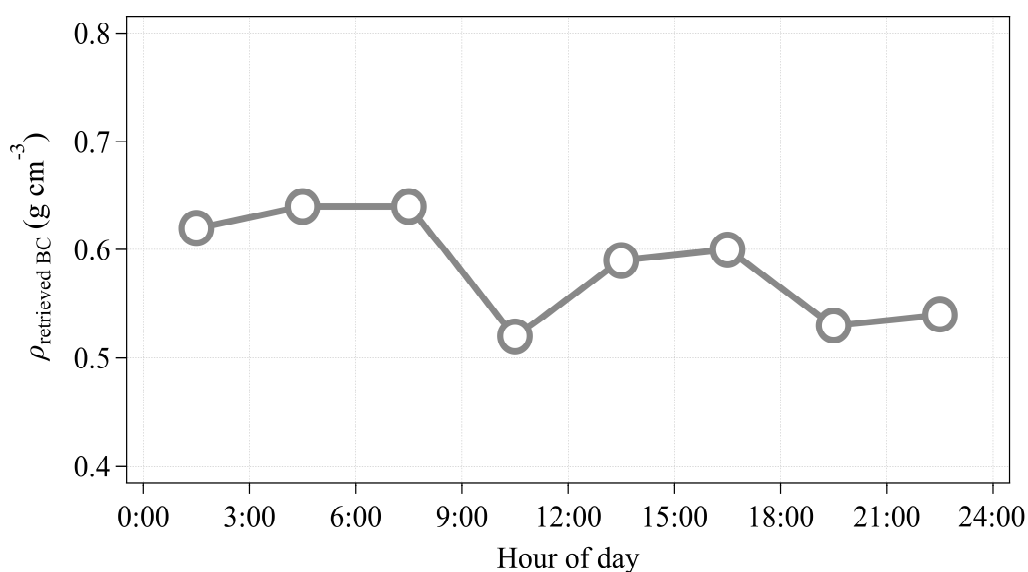


Figure R6 (S18). Diurnal variation of retrieved BC effective density.

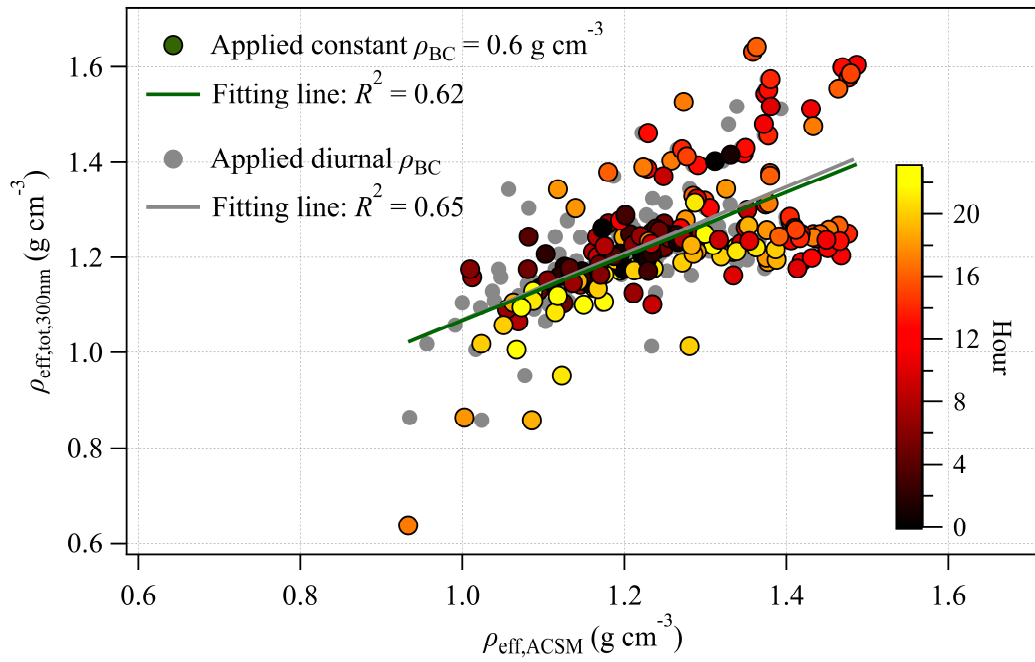


Figure R7 (S19). Comparison of the average effective density of particles at 300 nm observed by DMA-CPMA-CPC ($\bar{\rho}_{\text{eff,tot,300nm}}$) and ACSM-derived bulk effective density ($\rho_{\text{eff,ACSM}}$) by applied a constant ρ_{BC} or diurnal varied ρ_{BC} .

9. The conclusions should be shortened to be more concise, in particular, there are several numbers that are not really important.

Response:

Thanks for the comment. We have shortened and refined the conclusion in the revised manuscript.